

Pharmacokinetic/Pharmacodynamic Modelling of GnRH Antagonist Degarelix: A Comparison of the Non-linear Mixed-Effects Programs NONMEM and NLME

Christoffer W. Tornøe,^{1,*} Henrik Agersø,¹ Henrik A. Nielsen,² Henrik Madsen,² and E. Niclas Jonsson³

In this paper, the two non-linear mixed-effects programs NONMEM and NLME were compared for their use in population pharmacokinetic/pharmacodynamic (PK/PD) modelling. We have described the first-order conditional estimation (FOCE) method as implemented in NONMEM and the alternating algorithm in NLME proposed by Lindstrom and Bates. The two programs were tested using clinical PK/PD data of a new gonadotropin-releasing hormone (GnRH) antagonist degarelix currently being developed for prostate cancer treatment. The pharmacokinetics of intravenous administered degarelix was analysed using a three compartment model while the pharmacodynamics was analysed using a turnover model with a pool compartment. The results indicated that the two algorithms produce consistent parameter estimates. The bias and precision of the two algorithms were further investigated using a parametric bootstrap procedure which showed that NONMEM produced more accurate results than NLME together with the nlmeODE package for this specific study.

KEY WORDS: population pharmacokinetic/pharmacodynamic modelling; non-linear mixed-effects programs; NONMEM; NLME; degarelix; GnRH antagonist.

INTRODUCTION

Population pharmacokinetic/pharmacodynamic (PK/PD) data analysis using non-linear mixed effects models has become an increasingly

¹Experimental Medicine, Ferring Pharmaceuticals A/S, Kay Fiskers Plads 11, DK 2300, Copenhagen S, Denmark.

²Informatics and Mathematical Modelling, Technical University of Denmark, Lyngby, Denmark.

³Department of Pharmaceutical Biosciences, Division of Pharmacokinetics and Drug Therapy, Uppsala University, Uppsala, Sweden.

*To whom correspondence should be addressed. Tel: +45-2878-7453; Fax: +45-2817-6453; e-mail: christoffer.tornoe@ferring.com

important tool in all phases of drug development [1]. The advantage of using non-linear mixed-effects models are that population mean parameters are obtained simultaneously with estimates of the inter- and intra-individual variability. The available software for population PK/PD modelling have previously been reviewed in [2, 3] and extensively compared using simulated and clinical data in [4–7]. NONMEM [8] is by far the most applied program in population PK/PD modelling while the NLME package [9] has had limited use in that area so far. With the implementation of an ordinary differential equation (ODE) solver in nlmeODE [10] combining NLME and the odesolve package [11] in the statistical modelling environment R [12], it is now possible to use NLME for modelling complicated PK/PD systems for which closed-form solutions do not exist. This calls for a comparison between NONMEM and NLME using the nlmeODE package.

NONMEM and NLME are both parametric non-Bayesian likelihood approaches proposing different approximations of the population likelihood function. The first-order conditional estimation (FOCE) method in NONMEM is compared with the maximum likelihood (ML) method in the alternating algorithm proposed by Lindstrom and Bates as implemented in NLME since these seem to be the most similar [8]. Several other algorithms are available in NONMEM and NLME but these are not compared in this study.

The objectives of this study are: (1) to model the PK/PD of GnRH antagonist degarelix, (2) to compare the parameter estimates obtained from NONMEM and NLME, and (3) to identify the advantages and disadvantages of these two non-linear mixed-effects programs in population PK/PD modelling.

THEORETICAL

The statistical framework for non-linear mixed-effects modelling is presented in the following along with the first-order conditional estimation (FOCE) method as implemented in NONMEM [8] and the alternating algorithm in NLME proposed by Lindstrom and Bates [13].

NON-LINEAR MIXED-EFFECTS MODELLING

Population PK/PD data analysis is typically performed using non-linear mixed-effects models which allow for estimation of inter- and intra-individual variability (random effects) as well as the influence of measured concomitant effects or covariates on the fixed-effects parameters. To ease the notation, bold symbols refer to vector or matrix representation.

Non-linear mixed-effects models can be thought of as a hierarchical model structure where the variability in response is split into inter- and intra-individual variability. The likelihood method described below may only be used when there is a complete model for the probability distribution underlying the data. The hierarchical model consists of the following two-stage hierarchy [14,15].

The first-stage model describes the intra-individual (residual) variability and is modelled for each individual conditioned on the independent variables and a set of individual parameters, i.e.

$$p_1(\mathbf{y}_{ij}|\boldsymbol{\phi}_i, \boldsymbol{\Sigma}, \mathbf{x}_{ij}), \quad i = 1, \dots, N \quad j = 1, \dots, n_i \tag{1}$$

where $p_1(\cdot)$ is a generic probability density function, \mathbf{y}_{ij} is the j th response vector for the i th individual, $\boldsymbol{\phi}_i$ is the individual-specific parameter vector, $\boldsymbol{\Sigma}$ is the first-stage variance, \mathbf{x}_{ij} is a known regressor matrix, N is the number of individuals, and n_i is the number of measurements for individual i . To ease the exposition, we only consider univariate measurement with a homoscedastic residual error model, i.e.

$$y_{ij} = f(\boldsymbol{\phi}_i, \mathbf{x}_{ij}) + \epsilon_{ij} \tag{2}$$

where $f(\cdot)$ is the structural model and the error terms ϵ_{ij} are assumed independent and identically distributed residual errors with mean zero and variance $\boldsymbol{\Sigma} = \sigma^2$.

At the second-stage, the model relates the parameters of the different individuals, i.e.

$$p_2(\boldsymbol{\phi}_i|\boldsymbol{\theta}, \mathbf{z}_i), \quad i = 1, \dots, N \tag{3}$$

with the second-stage model commonly modelled as

$$\boldsymbol{\phi}_i = \mathbf{h}(\boldsymbol{\theta}, \mathbf{z}_i)\exp(\boldsymbol{\eta}_i) \tag{4}$$

where $\mathbf{h}(\cdot)$ denotes the structural type parameter model which is a function of the fixed-effects parameters $\boldsymbol{\theta}$, covariates \mathbf{z}_i , and random-effects parameters $\boldsymbol{\eta}_i$ influencing $\boldsymbol{\phi}_i$. This parameterization is chosen in order to constrain the parameters to be non-negative. The random-effects $\boldsymbol{\eta}_i$ are independent and identically distributed with zero mean and variance-covariance matrix $\boldsymbol{\Omega}$. The second-stage distribution $p_2(\cdot)$ is normally assumed to be the multivariate normal distribution and the two levels of random-effects ϵ_{ij} and $\boldsymbol{\eta}_i$ are assumed independent for all i and j .

The marginal density of $\mathbf{y}_i = [y_{i1}, \dots, y_{in_i}]$ is obtained from the conditional density of \mathbf{y}_i given the random effects $\boldsymbol{\eta}_i$ and the marginal distribution of $\boldsymbol{\eta}_i$, i.e.

$$p(y_i|\theta, \Sigma, \Omega) = \int p_1(y_i|\theta, \Sigma, \eta_i)p_2(\eta_i|\Omega)d\eta_i \tag{5}$$

where the conditional density of y_i given the random-effects η_i is denoted by $p_1(y_i|\theta, \Sigma, \eta_i)$ while $p_2(\eta_i|\Omega)$ is the marginal distribution of η_i [9].

The likelihood function for the population parameters based on the marginal density in (5) can be written as the following product of integrals [5,14,16]

$$\begin{aligned} L(\theta, \Sigma, \Omega) &= \prod_{i=1}^N \int p_1(y_i|\theta, \Sigma, \eta_i)p_2(\eta_i|\Omega)d\eta_i \\ &\propto \Sigma^{-\frac{M}{2}}|\Omega|^{-\frac{N}{2}} \prod_{i=1}^N \int \exp(-l_i)d\eta_i \end{aligned} \tag{6}$$

where

$$l_i = \frac{1}{2} \sum_{j=1}^{N_i} \left\{ \frac{(y_{ij} - f(\phi_i, \mathbf{x}_{ij}))^2}{\Sigma} \right\} + \frac{1}{2} \eta_i^T \Omega^{-1} \eta_i \tag{7}$$

with $M = \sum_{i=1}^N n_i$ being the total number of observations for the N individuals.

This formulation of the likelihood function is valid due to the fact that the empirical Bayes estimates $\hat{\eta}_i$ satisfy the following equation [17]

$$\frac{\partial l_i}{\partial \eta_i} \Big|_{\hat{\eta}_i} = 0, \quad i = 1, \dots, N \tag{8}$$

In general, the integral in (6) does not have a closed-form expression when the structural model function $f(\cdot)$ is non-linear in η and can therefore not be evaluated analytically [18]. Approximations therefore have to be made in order to be able to estimate the model parameters. The two likelihood approximations in NONMEM and NLME are therefore considered next.

FIRST-ORDER CONDITIONAL ESTIMATION METHOD IN NONMEM

The three main likelihood approximations available in NONMEM are the Laplacian approximation, the first-order conditional estimation (FOCE) method, and the first-order (FO) method listed in order of decreasing accuracy. The FOCE method in NONMEM of evaluating the exact marginal likelihood in (6) consists of using a second-order Taylor series expansion of l_i around the value of η_i which minimizes (7) [8].

Laplace’s approximation of the integral in (6) states that if l_i has a unique minimum at $\hat{\boldsymbol{\eta}}_i$ the integral in the likelihood function (6) can be approximated by using [17,19,20]

$$\int \exp(-l_i) d\boldsymbol{\eta}_i \approx (2\pi)^{k/2} |\Delta l_i|^{-1/2} \exp(-l_i) \tag{9}$$

where $\boldsymbol{\eta}_i$ is a k -dimensional random-effects vector and Δl_i is the Hessian matrix calculated by

$$\Delta l_i = \sum_{j=1}^{N_i} \frac{\nabla f(\boldsymbol{\phi}_i; \mathbf{x}_{ij}) \nabla f(\boldsymbol{\phi}_i; \mathbf{x}_{ij})^T}{\Sigma} + \boldsymbol{\Omega}^{-1} \tag{10}$$

with the gradient vector $\nabla f(\boldsymbol{\phi}_i; \mathbf{x}_{ij}) = \frac{\partial f}{\partial \boldsymbol{\eta}_i} \Big|_{\hat{\boldsymbol{\eta}}_i}$. Only first-order partial derivatives are included in (10) since the contribution of the second-order partial derivatives is negligible [18].

The objective function of the FOCE approximation thereby becomes

$$-2 \log L(\boldsymbol{\theta}, \boldsymbol{\Sigma}, \boldsymbol{\Omega}) \propto M \log \boldsymbol{\Sigma} + N \log |\boldsymbol{\Omega}| + \sum_{i=1}^N [\log |\Delta l_i| + 2l_i] \tag{11}$$

LINDSTROM AND BATES ALTERNATING ALGORITHM IN NLME

The method proposed by Lindstrom and Bates [13] for approximating the likelihood function in (5) is implemented in NLME [9,18]. The method uses a first-order Taylor expansion about the conditional estimates of the inter-individual random effects. The estimation algorithm alternates between two steps: A penalized non-linear least-squares (PNLS) step and a linear mixed-effects (LME) step.

In the PNLS step, the conditional modes of the random effects $\boldsymbol{\eta}_i$ and the conditional estimates of the fixed effects $\boldsymbol{\theta}$ based on the current estimate of $\boldsymbol{\Omega}$ are obtained by minimizing the PNLS objective function [18], i.e.

$$O_{\text{PNLS}} = \frac{1}{2} \sum_{i=1}^N \left\{ (\mathbf{y}_i - \mathbf{f}_i(\boldsymbol{\theta}, \boldsymbol{\eta}_i))^T \boldsymbol{\Sigma}^{-1} (\mathbf{y}_i - \mathbf{f}_i(\boldsymbol{\theta}, \boldsymbol{\eta}_i)) \right\} + \frac{1}{2} \boldsymbol{\eta}_i^T \boldsymbol{\Omega}^{-1} \boldsymbol{\eta}_i \tag{12}$$

where $[\mathbf{f}_i(\boldsymbol{\theta}, \boldsymbol{\eta}_i)]_j = f_i(\boldsymbol{\phi}_i; \mathbf{x}_{ij})$ for $i = 1, \dots, N$ and $j = 1, \dots, n_i$.

In order to update the estimate of $\boldsymbol{\Omega}$, the model function $f(\cdot)$ is linearized in the LME step using a first-order Taylor expansion around the current estimates of $\boldsymbol{\theta}$ and the conditional modes of the random effects $\boldsymbol{\eta}_i$ denoted by $\hat{\boldsymbol{\eta}}_i$ [18]. The approximative log-likelihood function for the estimation of $\boldsymbol{\Omega}$ in the LME step can thereby be written as

$$\log L_{\text{LME}}(\boldsymbol{\theta}, \Sigma, \boldsymbol{\Omega}) = -\frac{M}{2} \log 2\pi \Sigma - \frac{1}{2} \sum_{i=1}^N \left\{ \log \left(\Sigma + \frac{\partial f_i}{\partial \boldsymbol{\theta}^T} \boldsymbol{\Omega} \frac{\partial f_i}{\partial \boldsymbol{\theta}^T} \right) + \left[\mathbf{y}_i - \mathbf{f}_i(\boldsymbol{\theta}, \boldsymbol{\delta}_i) + \frac{\partial f_i}{\partial \boldsymbol{\eta}_i^T} \hat{\boldsymbol{\eta}}_i \right]^T \left(\Sigma + \frac{\partial f_i}{\partial \boldsymbol{\theta}^T} \boldsymbol{\Omega} \frac{\partial f_i}{\partial \boldsymbol{\theta}^T} \right)^{-1} \left[\mathbf{y}_i - \mathbf{f}_i(\boldsymbol{\theta}, \boldsymbol{\eta}_i) + \frac{\partial f_i}{\partial \boldsymbol{\eta}_i^T} \hat{\boldsymbol{\eta}}_i \right] \right\} \quad (13)$$

The log-likelihood function in (13) is identical to that of a linear mixed-effects model [21].

MATERIALS AND METHODS

Compound

Degarelix (FE200486, Ac-D-2Nal-D-4Cpa-D-3Pal-Ser-4Aph (L-hydroorotyl)-D-4Aph (carbmoyl)-Leu-ILys-Pio-D-Ala-NH₂) is a new long-acting GnRH antagonist with high affinity and selectivity for GnRH receptors currently being developed for prostate cancer treatment [22–26].

Experimental Design

The phase I study was designed as an open-label, escalating dose study with sequential intravenous treatment groups with 24 healthy male subjects enrolled in the study. The study was performed in accordance with the Declaration of Helsinki and according to Good Clinical Practice (GCP). The appropriate independent ethics committee approved the protocol prior to study initiation. Written informed consent was obtained from all patients prior to participation in the study.

Four treatment groups with six subjects in each received degarelix administered as an intravenous infusion at escalating doses of 1.5, 6, 15, and 30 µg/kg, respectively. The concentration of the infusion solution was 5 µg/ml and it was infused at a constant rate within each subject over a period of 15 min (for the 1.5 and 6 µg/kg groups) and over 45 min (for the 15 and 30 µg/kg groups).

Blood samples for assessment of degarelix were taken prior to dosing, three times during the infusion, and 5, 10, 15, 30, 45, 60 min, 2, 4, 8, 12, 24, 36, 48 h, 3, 4, 7, and 14 days after end of infusion. Blood samples for assessment of pharmacodynamic effect were taken prior to dosing, every 15 min during the infusion, and 15, 30, 60 min, 2, 4, 8, 12, 24, 48 h, 3, 4, 7, and 14 days after infusion stop.

Analytical Methods

Degarelix plasma concentrations and total serum testosterone concentrations were measured according to Good Laboratory Practice (GLP)

by liquid chromatography with tandem mass spectrometric detection (LC-MS/MS) validated according to current guidelines for bioanalytical samples [27].

The lower limit of quantification (LLOQ) of the degarelix assay was 0.5 µg/ml. The intra and inter-assay precision (expressed as coefficient of variation (CV)) were less than or equal to 7.5% and 14.1%, respectively. The accuracy was between 98.2% and 102.6%.

The LLOQ the testosterone assay was 0.05 ng/ml and the intra- and inter-assay precision were less than or equal to 15.8% and 14.1%, respectively. The accuracy was between 93.8% and 107.8%.

Mechanism of Action for GnRH Antagonists

The following is a brief description of the physiological aspects and mechanisms of the endocrine system with respect to the hypothalamic-pituitary-gonadal (HPG) axis on which gonadotropin-releasing hormone (GnRH) antagonist degarelix acts. Endogenous GnRH is secreted from neurons in the hypothalamus and acts as an agonist stimulating the synthesis and secretion of the gonadotropins luteinizing hormone (LH) and follicle-stimulating hormone (FSH) [28]. LH interacts with receptors on the plasma membrane of testicular Leydig cells which stimulate *de novo* synthesis of androgens [29,30].

Treatment with GnRH antagonists cause immediate suppression of gonadotropin secretion by binding to the GnRH receptors in the pituitary [31]. The blockage of gonadotropins causes suppression of *de novo* synthesis of androgens (primarily testosterone) in the Leydig cells on which the growth of prostate cancer cells depend [29,30,32]. Continuous blockade of the pituitary GnRH receptors by GnRH antagonists subsequently results in down-regulation of GnRH receptors followed by decreased sensitivity to endogenous GnRH [28].

Data Analysis

The population PK/PD data analysis was carried out using NONMEM version V with ADVAN8 [8] and NLME version 3.1–45 [9] on a Pentium 4-M 2.0 GHz computer with 512 MB RAM running Windows XP.

The fixed-effects parameters were parameterized in terms of the logarithm of the parameters to ensure non-negative parameter estimates while keeping the optimization problem unconstrained. This procedure was not

necessary in NONMEM but to be able to compare the results from NONMEM and NLME, it was used in both programs.

The precision of the parameter estimates was calculated using the inverse Hessian matrix thereby assuming asymptotic normality. Since the logarithm of the fixed-effects parameters were estimated, the relative standard error (RSE) estimate of the untransformed fixed-effect parameters θ were calculated by the following Taylor approximation

$$\text{RSE} = \frac{\text{SE}(\hat{\theta})}{\hat{\theta}} \approx \frac{\text{SE}(\log \hat{\theta}) \hat{\theta}}{\hat{\theta}} = \text{SE}(\log \hat{\theta}) \quad (14)$$

where $\text{SE}(\log \hat{\theta})$ are the reported standard error estimates.

The inter-individual variability (IIV) was estimated using an exponential model, i.e.

$$\phi_i = \theta \exp(\eta_i) \quad (15)$$

where ϕ_i denotes an arbitrary PK/PD parameter for individual i , θ is the corresponding population parameter while η_i is a normal distributed variable with variance ω_θ^2 to distinguish the i th subject's parameter from the population mean. The inter-individual variance matrix $\mathbf{\Omega}$ was specified as a diagonal matrix since the correlation among all pairs of η_i were assumed to be zero. The inter-individual variability was parameterized in terms of the coefficient of variation ω in both NONMEM and NLME in order to automatically get the asymptotic standard error estimates of ω instead of ω^2 .

A sequential approach for analysing the PK/PD data was chosen since the PD can be assumed not to influence the PK because degarelix is an exogenous compound. First, the individual (empirical Bayes) PK parameters were estimated using the PK data alone. Secondly, using the individual PK parameters and the PD data only, the PD parameters were estimated. This approach is referred to as the individual PK parameters (IPP) method in [33].

RESULTS

Pharmacokinetics

The pharmacokinetics of degarelix following a single intravenous infusion was adequately described by a three-compartment disposition model with first-order elimination from the central compartment in equilibrium with two peripheral compartments (see Fig. 1). The differential equations governing the structural PK model are

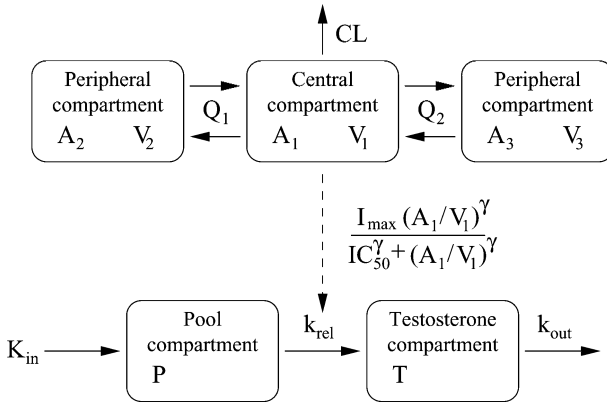


Fig. 1. Schematic illustration of the structural PK/PD model for GnRH antagonist degarelix. The solid lines illustrate mass transfer while the dashed line represents effect interaction. The parameters are explained in the text.

$$\frac{dA_1}{dt} = \frac{Q_1}{V_2} A_2 + \frac{Q_2}{V_3} A_3 - \frac{CL + Q_1 + Q_2}{V_1} A_1 + R_{in} \tag{16}$$

$$\frac{dA_2}{dt} = Q_1 \left(\frac{A_1}{V_1} - \frac{A_2}{V_2} \right) \tag{17}$$

$$\frac{dA_3}{dt} = Q_2 \left(\frac{A_1}{V_1} - \frac{A_3}{V_3} \right) \tag{18}$$

where A_1 , A_2 , and A_3 are the state variables for the amount of drug in the central and the two peripheral compartments, respectively, with the corresponding volumes V_1 , V_2 and V_3 . The inter-compartmental clearance parameters are Q_1 and Q_2 while CL is the clearance and R_{in} is the IV infusion rate. The IIV model in (15) was applied to CL , Q_1 , and V_1 . No demographic covariates were found to be significant by graphical analysis using Xpose [34] and were therefore not included in the final model.

To obtain homogeneity of the residual error variance for the PK data analysis, the intra-individual variability was modelled using an additive residual error model on the log-scale corresponding to a constant coefficient of variation (CV) model on the untransformed scale, i.e.

$$\log C_{ij}^{PK} = \log \frac{A_{1,ij}}{V_{1,i}} + \epsilon_{ij}^{PK} \tag{19}$$

where C_{ij}^{PK} is the j th observed plasma degarelix concentration for individual i and ϵ^{PK} are the residuals which are independent and identically distributed (iid) with mean zero and variance σ_{PK}^2 .

The population PK parameter estimates obtained by NONMEM and NLME are summarized in Table I. The NONMEM and NLME parameter estimates were quite similar while the discrepancy in the RSE estimates was a bit higher. The bias and precision were investigated further using a parametric bootstrap procedure (see the Parametric Bootstrapping section).

The observed degarelix concentration-time profiles are shown in Fig. 2 together with the model predictions. The goodness-of-fit (GOF) graphs of observed versus individual predicted and population predicted plasma degarelix concentrations are displayed in Fig. 3. The GOF graphs show that the NONMEM and NLME PK model predictions are almost identical and that a three-compartment PK model seems to capture the pharmacokinetics of IV administered degarelix since the circles in Fig. 3 are nicely scattered around the line of identity.

Pharmacodynamics

To model the testosterone system following exposure to GnRH antagonist degarelix, a turnover model with a pool compartment [35,36]

Table I. Population PK/PD Parameter Estimates Obtained from NONMEM and NLME Together with their Relative Standard Error (RSE) Estimates

| Parameter | Unit | NONMEM | | NLME | |
|------------------------------|---------|----------|------------------------|----------|------------------------|
| | | Estimate | (RSE ^a (%)) | Estimate | (RSE ^a (%)) |
| CL | [l/h] | 3.29 | (4.01) | 3.29 | (4.94) |
| Q ₁ | [l/h] | 2.57 | (12.4) | 2.91 | (10.6) |
| Q ₂ | [l/h] | 10.7 | (14.9) | 10.9 | (3.05) |
| V ₁ | [l] | 9.78 | (6.99) | 9.64 | (6.64) |
| V ₂ | [l] | 31.8 | (4.75) | 32.3 | (4.74) |
| V ₃ | [l] | 8.85 | (10.5) | 7.74 | (6.75) |
| k _{out} | [1/h] | 0.217 | (4.82) | 0.213 | (5.08) |
| k _{rel} | [1/h] | 0.00224 | (37.2) | 0.00320 | (34.9) |
| I _{max} | [-] | 0.948 | (0.580) | 0.958 | (0.601) |
| IC ₅₀ | [ng/ml] | 0.696 | (12.4) | 0.683 | (15.7) |
| γ | [-] | 3.03 | (11.2) | 2.30 | (5.97) |
| ω _{CL} | [%] | 17.6 | (17.3) | 20.6 | (22.1) |
| ω _{Q₁} | [%] | 30.8 | (33.0) | 46.9 | (24.8) |
| ω _{V₁} | [%] | 27.7 | (17.7) | 31.5 | (19.6) |
| ω _{k_{out}} | [%] | 18.5 | (20.0) | 19.1 | (25.0) |
| ω _{IC₅₀} | [%] | 54.5 | (15.2) | 54.1 | (20.3) |
| σ _{PK} | [%] | 19.8 | (4.22) | 20.2 | (4.29) |
| σ _{PD} | [%] | 23.8 | (4.02) | 23.9 | (4.16) |

^aRSE of fixed-effects estimates are calculated by $RSE(\hat{\theta}) \approx SE(\log \hat{\theta})$.

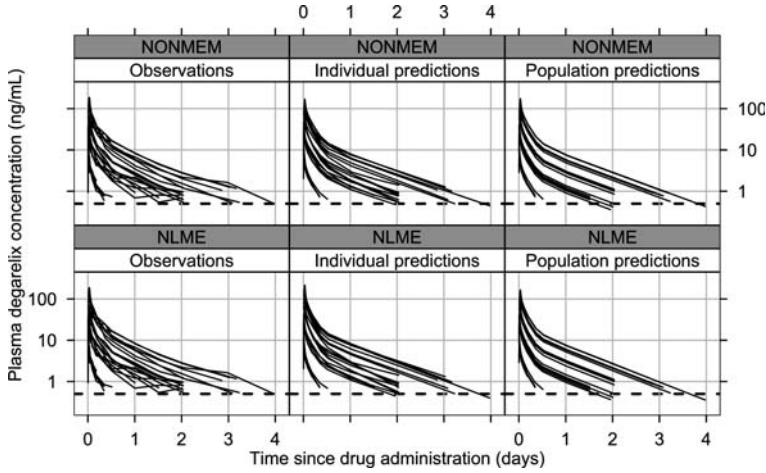


Fig. 2. Observed and predicted plasma degarelix concentration-time profiles plotted on a semi-logarithmic scale with each line representing data from one individual. NONMEM (Top), NLME (Bottom), observed data (Left), individual predictions (Middle), and population predictions (Right). The dashed lines represent the lower limit of quantification (LLOQ) of 0.5 ng/ml for the degarelix assay.

(see Fig. 1) was considered the most appropriate given the available data and the current knowledge about the system. The observed rebound effect where the testosterone concentration levels rise above the baseline concentration was accounted for by adding a pool compartment representing intracellular testosterone. The release of intracellular testosterone to the plasma testosterone compartment is thought to be inhibited by plasma degarelix concentrations through a sigmoidal E_{max} model. The down-regulation of GnRH receptors was not modelled since the extent of exposure to degarelix is limited in the current study.

The differential equations governing the structural PD model are

$$\frac{dP}{dt} = K_{in} - k_{rel} \left(1 - \frac{I_{max}(A_1/V_1)^\gamma}{IC_{50}^\gamma + (A_1/V_1)^\gamma} \right) P \tag{20}$$

$$\frac{dT}{dt} = k_{rel} \left(1 - \frac{I_{max}(A_1/V_1)^\gamma}{IC_{50}^\gamma + (A_1/V_1)^\gamma} \right) P - k_{out} T \tag{21}$$

where P and T are the state variables for the intracellular pool and testosterone concentrations, respectively. The PD model parameters are K_{in} (zero-order rate constant for production of P), k_{rel} (first-order rate-constant for release of P), k_{out} (first-order rate constant for elimination of testosterone), I_{max} (maximal inhibiting effect constrained to be less than

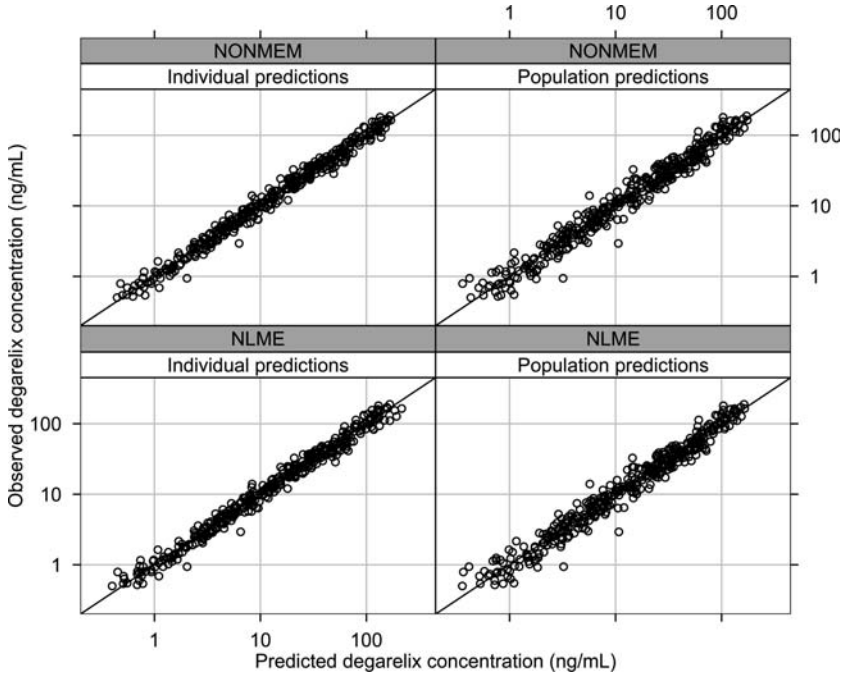


Fig. 3. Observed versus individual predicted (Left) and population predicted (Right) plasma degarelix concentrations plotted on a double-logarithmic scale. NONMEM (Top) and NLME (Bottom) results. The solid lines are the lines of identity.

or equal to 1), IC_{50} (plasma degarelix concentration producing 50% of maximal inhibiting effect), and γ (sigmoidicity factor). IIV was estimated for k_{out} and IC_{50} .

By assuming steady-state before drug administration, the initial conditions for the system of differential Eqs. in (20) and (21) were specified by

$$P_0 = \frac{K_{in}}{k_{rel}} \quad (22)$$

$$T_0 = \frac{K_{in}}{k_{out}} \quad (23)$$

The initial testosterone concentration T_0 was set equal the observed testosterone baseline at $t=0$ h while removing this observation from the data used for the estimation. The parameter K_{in} was therefore reparameterized using the relationship in (23), i.e. $K_{in} = k_{out}T_0$. Attempts were made to estimate the testosterone baseline but without success.

The observation equation for the PD data analysis of testosterone is

$$\log C_{ij}^{PD} = \log T_{ij} + \epsilon_{ij}^{PD} \tag{24}$$

where the residuals ϵ^{PD} are *iid* with mean zero and variance σ_{PD}^2 .

The population PD parameter estimates obtained from NONMEM and NLME are summarized in Table I. The discrepancy between the NONMEM and NLME PD parameter estimates was a bit higher than what was observed for the PK parameters. Especially the relative difference in the NONMEM and NLME parameter estimates of k_{rel} and γ was approximately 30% and 25%, respectively.

The concentration-time profiles of observed and predicted testosterone concentrations are illustrated in Fig. 4 while the GOF graphs of observed versus predicted testosterone concentrations are displayed in Fig. 5.

IV administration of degarelix resulted in a rapid decrease in testosterone concentrations of all treated subjects and castration levels (testosterone concentrations below 0.5 ng/ml) were reached within 24 h. The duration of testosterone suppression was up to 48 h whereafter a rebound effect was observed where the testosterone concentration rises

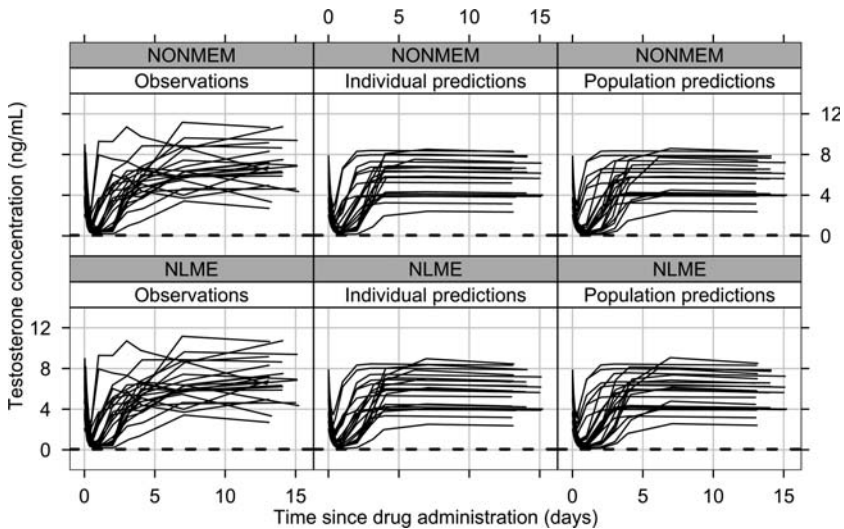


Fig. 4. Observed and predicted testosterone concentration-time profiles with each line representing data from one individual. NONMEM (Top), NLME (Bottom), observed data (Left), individual predictions (Middle), and population predictions (Right). The dashed lines represent the lower limit of quantification (LLOQ) of 0.05 ng/ml for the testosterone assay.

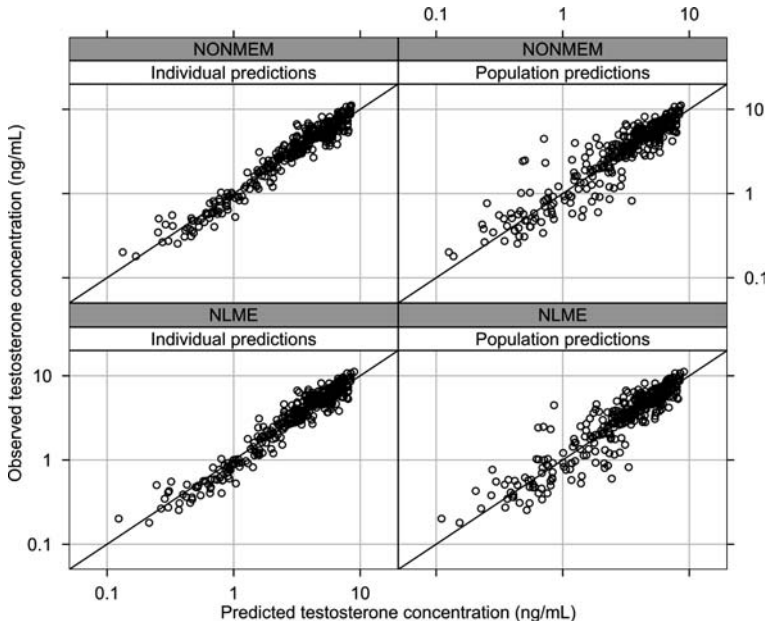


Fig. 5. Observed versus individual predicted (Left) and population predicted (Right) testosterone concentrations plotted on a double-logarithmic scale. NONMEM (Top) and NLME (Bottom) results. The solid lines are the lines of identity.

above the initial concentration and eventually returns to the baseline. The turnover model with an intracellular pool did not fully capture the increase in testosterone concentrations above baseline (see Figs. 4 and 5) but was otherwise adequate at describing the testosterone concentration-time profile following short time exposure to GnRH antagonist degarelix.

Parametric Bootstrapping

NONMEM and NLME were further compared using a parametric bootstrap procedure [37] to evaluate the bias and precision of the obtained parameter estimates.

The PK/PD model which was used to analyse the clinical PK/PD data of degarelix was used for simulating 100 data sets with the same data design as the original data. The average of the original population PK/PD parameter estimates from NONMEM and NLME were used for

the simulation. The simulated data sets were analysed in NONMEM and NLME using the same model as was used for the simulation.

The sample mean and relative standard deviation (RSD) estimates of the 100 parametric bootstrap replicates from NONMEM and NLME are reported in Table II along with the parameter values used for the simulation. The sample RSD estimates from the parametric bootstrap procedure were noticeably more alike between the two programs than the asymptotic RSE estimates reported in Table I.

To compare the bias of the obtained parameter estimates, the sample mean bootstrapped parameter estimates are plotted in Fig. 6 together with a 95% percentile interval (using the non-parametric bootstrap percentile method with 10,000 bootstrap replications [37]) and the parameter values used for the simulation. Three of the 18 parameters from NONMEM and 10 of the parameters from NLME are significantly different from their simulated parameter values on a 5% significance level. There seems to be a pattern in the parameter estimates of Q_1 and V_2 which are larger in NLME compared to NONMEM while the opposite is true for Q_2 and V_3 .

Table II. Empirical Mean Population PK/PD Parameter Estimates and Relative Standard Deviation (RSD) Estimates from NONMEM and NLME of 100 Bootstrap Replicates

| Parameter | Unit | Simulated | NONMEM | | NLME | |
|--------------------|---------|-----------|---------|------------------------|---------|------------------------|
| | | | Mean | (RSD ^a (%)) | Mean | (RSD ^a (%)) |
| CL | [l/h] | 3.29 | 3.30 | (4.54) | 3.31 | (4.84) |
| Q_1 | [l/h] | 2.74 | 2.69 | (11.1) | 2.91 | (12.0) |
| Q_2 | [l/h] | 10.8 | 11.1 | (13.8) | 10.7 | (8.56) |
| V_1 | [l] | 9.71 | 9.61 | (6.88) | 9.59 | (6.41) |
| V_2 | [l] | 32.1 | 31.7 | (5.05) | 32.9 | (5.50) |
| V_3 | [l] | 8.30 | 8.56 | (8.01) | 8.23 | (9.38) |
| k_{out} | [1/h] | 0.215 | 0.214 | (4.40) | 0.214 | (4.40) |
| k_{rel} | [1/h] | 0.00271 | 0.00261 | (43.1) | 0.00195 | (50.1) |
| I_{max} | [-] | 0.953 | 0.953 | (0.529) | 0.951 | (0.530) |
| IC ₅₀ | [ng/ml] | 0.688 | 0.668 | (15.8) | 0.725 | (15.7) |
| γ | [-] | 2.67 | 2.63 | (10.0) | 2.96 | (11.7) |
| ω_{CL} | [%] | 19.1 | 19.5 | (18.4) | 19.8 | (18.2) |
| ω_{Q_1} | [%] | 38.9 | 38.0 | (23.0) | 32.5 | (20.7) |
| ω_{V_1} | [%] | 29.6 | 28.3 | (17.8) | 26.5 | (25.3) |
| $\omega_{k_{out}}$ | [%] | 18.9 | 18.3 | (21.4) | 18.4 | (21.1) |
| ω_{IC50} | [%] | 54.3 | 53.9 | (18.5) | 49.6 | (21.4) |
| σ_{PK} | [%] | 20.0 | 19.9 | (3.86) | 20.4 | (4.23) |
| σ_{PD} | [%] | 23.8 | 23.7 | (4.38) | 23.8 | (4.43) |

^aRSD of bootstrapped fixed-effects estimates $\hat{\theta}_b$ are calculated by $RSD(\hat{\theta}_b) \approx SD(\log \hat{\theta}_b)$.

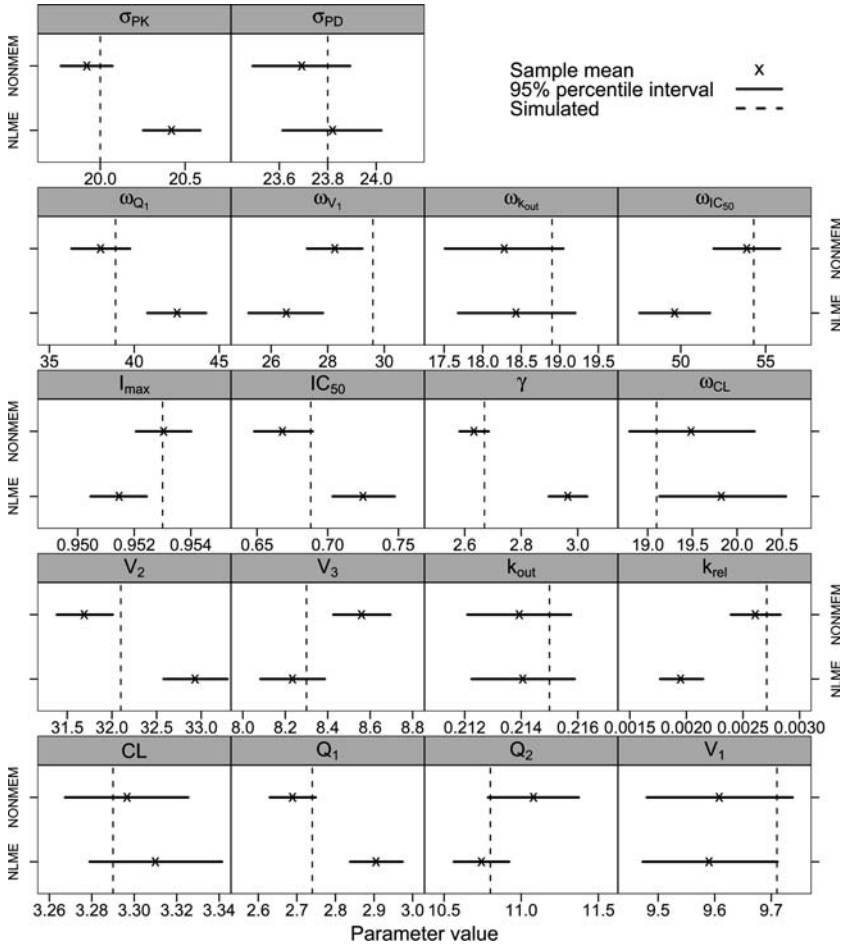


Fig. 6. Comparison of the simulated parameter values and the sample mean parameter estimates of the 100 parametric bootstrap replicates from NONMEM and NLME.

The precision of the bootstrapped parameter estimates was finally investigated by comparing the sample RSD estimates with the mean asymptotic RSE estimates of the 100 bootstrap replicates (see Fig. 7). The mean asymptotic RSE estimates seemed to underpredict the sample RSD estimates and the discrepancy between the RSD and RSE estimates was noticeably higher in NLME compared to NONMEM.

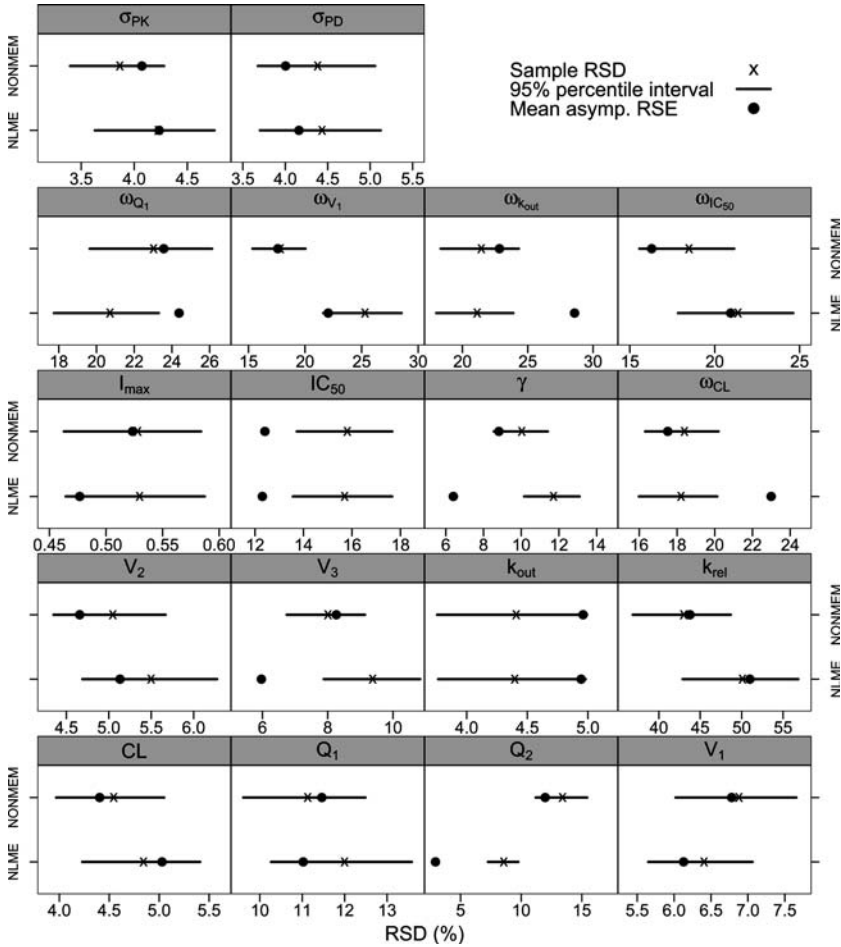


Fig. 7. Comparison of the sample RSD estimates with the mean asymptotic RSE estimates of the 100 parametric bootstrap replicates.

DISCUSSION

In the present analysis, the main objective was to compare the two non-linear mixed-effects algorithms implemented in NONMEM and NLME using clinical PK/PD data of GnRH antagonist degarelix and to investigate the pro’s and con’s of the two programs.

The estimation of parameters in non-linear mixed-effects models is a difficult statistical problem where no exact closed-form solution to the

population likelihood function exists. We have described and compared two approximations to the likelihood function, i.e. the FOCE method and Lindstrom and Bates alternating algorithm as implemented in NONMEM and NLME, respectively. In [18], it is concluded that the FOCE method (equivalent to what is called the modified Laplacian method in [18]) is generally more accurate than Lindstrom and Bates alternating algorithm since the FOCE method uses an expansion around the estimated random effects only and not like the LME approximation in NLME which makes it around both the estimated fixed and random effects. The alternating algorithm is though supposed to be less computer intensive than the FOCE method because the PNLs step can be solved for all individuals simultaneously and since the objective function can be profiled on the fixed effects [18].

In this particular study, the obtained parameter and relative standard error estimates for the clinical PK/PD data of degarelix were consistent between NONMEM and NLME with a few exceptions. Both methods required approximately the same number of function evaluations but the computation times were significantly longer using NLME together with nlmeODE compared to NONMEM. This is most likely due to the implementation of NLME and nlmeODE in R which is an interpreted language while NONMEM is written in Fortran which is a compiled language. The results indicated that the two likelihood approximations in NONMEM and NLME yield similar parameter estimates when analysing complicated PK/PD models without closed-form solutions.

The two programs were further compared using a parametric bootstrap procedure in order to evaluate the bias and precision of the obtained parameter estimates. The results indicated that the accuracy of the FOCE method is higher than that of Lindstrom and Bates alternating algorithm in this specific study. Furthermore, if one wish to obtain reliable estimates of the parameter uncertainty, one should consider to use likelihood profiling or a bootstrapping procedure instead of using the asymptotic RSE estimates reported in NONMEM and NLME. The 100 parametric bootstrap replicates were found adequate for evaluating the bias and precision of the two programs taking into account the available time and computer power. Furthermore, as indicated by the results, the number of bootstrap replicates was high enough to draw conclusions regarding bias and precision.

NONMEM is currently the most extensively applied non-linear mixed-effects program in population PK/PD modelling while NLME has had limited use since it previously has not been possible to estimate parameters in models without closed-form solutions. With the nlmeODE package [10], it is now possible to specify differential equations in NLME

Table III. Identified Advantages and Disadvantages of NLME Compared to NONMEM

-
- Advantages
 - No data set modification necessary for specifying initial concentrations.
 - Possible to obtain predictions at other time points than those used for estimation without modifying the data set.
 - Easy to specify variance and correlation structures in the residual errors using pre-programmed functions.
 - Implemented as part of the free statistical software environment R.
 - Tools for graphical analysis of the fitted model available within R.
 - Statistical tests for model comparison/validation and parameter distribution are implemented in NLME.
 - Disadvantages
 - It is not possible to specify parameter boundaries on fixed-effects parameters.
 - Simplified likelihood approximation like the FO method not available.
 - The parameterization of the intra-individual variability model cannot be specified using equations in NLME and it is quite complicated to construct new variance functions.
 - Inter-individual variability can only be modelled as additive or exponential.
 - NLME is not as well tested in population PK/PD modelling as NONMEM.
-

using a similar syntax as used in NONMEM. The identified advantages and disadvantages of NLME compared to NONMEM are summarized in Table III. In general, NONMEM seems to be superior in accuracy, stability, flexibility, and speed compared to NLME but when performing graphical and statistical data analysis, NLME is preferred over NONMEM.

In conclusion, this study demonstrated the use of NLME in population PK/PD modelling and compared it with NONMEM. The two non-linear mixed-effects programs were compared using clinical PK/PD data of GnRH antagonist degarelix. The PK/PD of IV administered degarelix was modelled using a three-compartment PK model and a turnover model with plasma degarelix concentrations inhibiting the release of testosterone from an intracellular pool. The obtained PK and PD parameter estimates were consistent between the FOCE method in NONMEM and Lindstrom and Bates alternating algorithm in NLME. Further comparison of the two algorithms using simulated data illustrated that NONMEM was more accurate than NLME for this specific example. Finally, the strengths and limitations of NLME compared to NONMEM in PK/PD modelling were identified. The comparison revealed that NLME should not be considered as a replacement for NONMEM but perhaps more as an alternative.

ACKNOWLEDGMENTS

This work was sponsored by Ferring Pharmaceuticals A/S, Denmark, the Swedish foundation for strategic research, Sweden, and Center for Information Technology, Denmark.

REFERENCES

1. L. Aarons, M. O. Karlsson, F. Mentre, F. Rombout, J. L. Steimer, and A. van Peer. Role of modelling and simulation in Phase I drug development. *Eur. J. Pharm. Sci.* **13**(2):115–122 (2001).
2. L. Yuh, S. Beal, M. Davidian, F. Harrison, A. Hester, K. Kowalski, E. Vonesh, and R. Wolfinger. Population pharmacokinetic/pharmacodynamic methodology and applications: a bibliography. *Biometrics* **50**(2):566–575 (1994).
3. L. Aarons. Software for population pharmacokinetics and pharmacodynamics. *Clin. Pharmacokinet.* **36**(4):255–264 (1999).
4. P. Maire, X. Barbaut, P. Girard, A. Mallet, R. W. Jelliffe, and T. Berod. Preliminary results of three methods for population pharmacokinetic analysis (NONMEM, NPML, NPEM) of amikacin in geriatric and general medicine patients. *Int. J. Biomed. Comput.* **36**(1–2):139–141 (1994).
5. J. E. Bennett and J. C. Wakefield. A comparison of a Bayesian population method with two methods as implemented in commercially available software. *J. Pharmacokinet. Biopharm.* **24**(4):403–432 (1996).
6. D. J. Roe. Comparison of population pharmacokinetic modeling methods using simulated data: results from the Population Modeling Workgroup. *Stat. Med.* **16**(11):1241–1257 (1997).
7. C. E. Staatz and S. E. Tett. Comparison of two population pharmacokinetic programs, NONMEM and P-PHARM, for tacrolimus. *Eur. J. Clin. Pharmacol.* **58**(9):597–605 (2002).
8. S. L. Beal and L. B. Sheiner. *NONMEM User's Guides*. NONMEM Project Group, University of California, San Francisco, 1994.
9. J. C. Pinheiro and D. M. Bates. *Mixed-Effects Models in S and S-PLUS*. Springer-Verlag, New York, 2000.
10. C. W. Tornøe, H. Agero, E. N. Jonsson, H. Madsen, and H. A. Nielsen. Non-linear mixed-effects pharmacokinetic/pharmacodynamic modelling in NLME using differential equations. *Comput. Methods Programs Biomed.* **76**(1):31–40 (2004).
11. R. W. Setzer. The odesolve Package version 0.5–8. Solvers for Ordinary Differential Equations. <http://www.cran.r-project.org>.
12. R Development Core Team. *R: A language and environment for statistical computing*. R Foundation for Statistical Computing, Vienna, Austria (2004). <http://www.R-project.org>.
13. M. J. Lindstrom and D. M. Bates. Nonlinear mixed effects models for repeated measures data. *Biometrics* **46**(3):673–687 (1990).
14. A. Racine-Poon and J. Wakefield. Statistical methods for population pharmacokinetic modelling. *Stat. Methods Med. Res.* **7**(1):63–84 (1998).
15. L. Sheiner and J. Wakefield. Population modelling in drug development. *Stat. Methods Med. Res.* **8**(3):183–193 (1999).
16. S. L. Beal and L. B. Sheiner. Estimating population kinetics. *Crit. Rev. Biomed. Eng.* **8**(3):195–222 (1982).
17. M. Davidian and D. M. Giltinan. *Nonlinear Models for Repeated Measurement Data*. Chapman & Hall, London, 1995.
18. J. C. Pinheiro and D. M. Bates. Approximations to the log likelihood function in the nonlinear mixed effects model. *J. Comput. Graph. Stat.* **4**(1):12–35 (1995).
19. R. Wolfinger. Laplace's approximation for nonlinear mixed models. *Biometrika* **80**:791–795 (1993).

20. E. F. Vonesh. A note on the use of Laplace's approximation for nonlinear mixed-effects models. *Biometrika* **83**(2):447–452 (1996).
21. M. J. Lindstrom and D. M. Bates. Newton-Raphson and EM Algorithms for Linear Mixed-Effects Models for Repeated-Measures Data. *J. Am. Stat. Assoc.* **83**(404):1014–1022 (1988).
22. G. Jiang, J. Stalewski, R. Galyean, J. Dykert, C. Schteingart, P. Broqua, A. Aebi, M. L. Aubert, G. Semple, P. Robson, K. Akinsanya, R. Haigh, P. Riviere, J. Trojnar, J. L. Junien, and J. E. Rivier. GnRH antagonists: a new generation of long acting analogues incorporating p-ureido-phenylalanines at positions 5 and 6. *J. Med. Chem.* **44**(3):453–467 (2001).
23. G.de Pinieux, M. E. Legrier, F. Poirson-Bichat, Y. Courty, R. Bras-Goncalves, A. M. Dutrillaux, F. Nemati, S. Oudard, R. Lidereau, P. Broqua, J. L. Junien, B. Dutrillaux, and M. F. Poupon. Clinical and experimental progression of a new model of human prostate cancer and therapeutic approach. *Am. J. Pathol.* **159**(2):753–764 (2001).
24. P. Broqua, P. J. Riviere, P. M. Conn, J. E. Rivier, M. L. Aubert, and J. L. Junien. Pharmacological profile of a new, potent, and long-acting gonadotropin-releasing hormone antagonist: degarelix. *J. Pharmacol. Exp. Ther.* **301**(1):95–102 (2002).
25. H. Agerso, W. Koechling, M. Knutsson, R. Hjortkjaer, and M. O. Karlsson. The dosing solution influence on the pharmacokinetics of degarelix, a new GnRH antagonist, after s.c. administration to beagle dogs. *Eur. J. Pharm. Sci.* **20**(3):335–340 (2003).
26. C. W. Tornoe, H. Agerso, H. A. Nielsen, H. Madsen, and E. N. Jonsson. Population Pharmacokinetic Modelling of a Subcutaneous Depot for GnRH Antagonist Degarelix. *Pharm. Res.* **21**(4):574–584 (2004).
27. V. P. Shah, K. K. Midha, S. Dighe, I. J. McGilveray, J. P. Skelly, A. Yacobi, T. Layloff, C. T. Viswanathan, C. E. Cook, and R. D. McDowall. Analytical methods validation: bioavailability, bioequivalence and pharmacokinetic studies. Conference report. *J. Drug Metab Pharmacokinet.* **16**(4):249–255 (1991).
28. D. Klingmuller and H. U. Schweikert. Gonadotropin-releasing hormone: physiological and endocrinological aspects. *Recent Results Cancer Res.* **124**:1–6 (1992).
29. K. L. Parker and B. P. Schimmer. *Pituitary Hormones and their Hypothalamic Releasing Factors. In Goodman & Gilman's The Pharmacological Basis of Therapeutics.* McGraw-Hill, London (2001).
30. J. E. Griffin and J. D. Wilson. *Disorders of the Testes and the Male Reproductive Tract. In Williams Textbook of Endocrinology.* W. B. Saunders Company, London (1992).
31. T. Cook and W. P. Sheridan. Development of GnRH antagonists for prostate cancer: new approaches to treatment. *The Oncologist* **5**(2):162–168 (2000).
32. A. J. Tilbrook and I. J. Clarke. Negative feedback regulation of the secretion and actions of gonadotropin-releasing hormone in males. *Biol. Reprod.* **64**(3):735–742 (2001).
33. L. Zhang, S. L. Beal, and L. B. Sheiner. Simultaneous vs. Sequential Analysis for Population PK/PD Data I: Best-case Performance. *J. Pharmacokinetic. Pharmacodyn.* **30**(6):387–404 (2003).
34. E. N. Jonsson and M. O. Karlsson. Xpose—an S-PLUS based population pharmacokinetic/pharmacodynamic model building aid for NONMEM. *Comput. Methods Programs Biomed.* **58**(1):51–64 (1999).
35. A. Sharma, W. F. Ebling, and W. J. Jusko. Precursor-dependent indirect pharmacodynamic response model for tolerance and rebound phenomena. *J. Pharm. Sci.* **87**(12):1577–1584 (1998).
36. M. Gardmark, L. Brynne, M. Hammarlund-Udenaes, and M. O. Karlsson. Interchangeability and predictive performance of empirical tolerance models. *Clin. Pharmacokinetic.* **36**(2):145–167 (1999).
37. B. Efron and R. Tibshirani. *An Introduction to the Bootstrap.* Chapman & Hall, London, 1993.